




 Cite this: *New J. Chem.*, 2023, 47, 5164

 Received 9th December 2022,
Accepted 2nd February 2023

DOI: 10.1039/d2nj06030b

rsc.li/njc

The promoting effect of boron oxide on the FeO_x/Si₃N₄ catalyst for oxidative dehydrogenation of ethylbenzene†

 Jian Sheng, Wen-Cui Li,  Bai-Chuan Zhou, Xin-Qian Gao, Bin Qiu, Wen-Duo Lu, Rui-Ping Zhang and An-Hui Lu *

Here, we report a visible promotion effect of the B₂O₃ additive on FeO_x/Si₃N₄ catalysts in the oxidative dehydrogenation of ethylbenzene. The oxygen reactivity of FeO_x was alleviated by the strong interaction between FeO_x and BO_x species, which suppresses the overoxidation of ethylbenzene and styrene to carbon oxides, thus promoting styrene selectivity.

Styrene (ST), one of the most important raw materials in the petrochemical industry, is mainly produced by the direct dehydrogenation (DH) of ethylbenzene (EB) process over K₂O-promoted Fe₂O₃ catalysts.^{1–4} Given the endothermic reaction nature of this process, high reaction temperature (600–650 °C) and excess superheated steam diluent (80–90 vol%) are needed to maintain an acceptable conversion (~60%) and mitigate the catalyst deactivation, which is against the agreement of green and sustainable development in the modern chemical industry.^{5–8} Oxidative dehydrogenation (ODH) of ethylbenzene featuring no conversion limitation from thermodynamics, lower operation temperature (400–500 °C), and no superheated steam input is an eco-friendly alternative to the direct dehydrogenation process.⁹ However, overoxidation of styrene or ethylbenzene to carbon oxides will be prevalent at high conversion, lowering the selectivity of styrene, especially catalysed by the reducible metal oxide catalysts.¹⁰ The lattice oxygen of reducible metal oxide catalysts plays an important role in the ODH of EB, including reduction (by EB) and reoxidation (by O₂) of the catalysts.¹¹ Among them, the reoxidation of the catalysts, namely the replenishment of lattice oxygen in the oxide from gas oxygen, has been considered a faster and more unmanageable step than the reduction step, usually causing the overoxidation reactions.¹² Thus, it is urgent to develop a catalyst

with manageable oxygen reactivity to achieve higher styrene selectivity.

Using additives to modify the interaction between the active phase and carrier of supported catalysts is an effective approach to altering the chemical state of the active phase and hence affecting the catalyst activity.¹³ For example, alkali cation additives can modulate the state and dispersion of nickel, cobalt, and molybdenum supported on alumina and silicon oxide.^{13,14} Besides, acidic B₂O₃ additive also reduces the reducibility and promotes the dispersion of Ni metal for Ni/γ-Al₂O₃ catalysts, attributed to the strong interaction between surface nickel and boron oxide, which exhibits excellent catalytic stability for steam methane reforming and dry methane reforming.^{15,16} Our previous work demonstrates that boron oxide (BO_x) species stemming from the boron nitride support could form stronger interaction with FeO_x species and further mitigate the oxygen of FeO_x species for higher styrene selectivity in oxidative dehydrogenation of ethylbenzene.⁸ However, it is difficult to quantify the actual amount of the *in situ* generated BO_x species from the BN support and further correlate its structure–performance relationship. Thus, it is essential to study the structure–performance correlation of the B₂O₃-modified FeO_x-based catalyst for the oxidative dehydrogenation of ethylbenzene with a definite amount of B₂O₃.

Here, to better quantitatively correlate the structure–performance relationship, a stable and inert silicon nitride (Si₃N₄, denote as SiN) material that possesses high thermal stability and thermal conductivity as well as oxidation and corrosion resistance^{17–19} is used as a support. A series of B₂O₃-modified FeO_x/SiN and boron-free catalysts were prepared for the oxidative dehydrogenation of ethylbenzene. These catalysts were further deeply characterized by various techniques including XRD, UV-vis DRS, TEM, H₂-TPR, CH₃OH-TPD, and XPS. The structure–performance relationship of these B₂O₃-modified FeO_x/SiN catalysts in the oxidative dehydrogenation of ethylbenzene was discussed in detail.

As shown in Fig. 1a and b, modification of boric oxide in 1FeO_x/SiN catalysts with the loading of B₂O₃ ranging from 0.1

State Key Laboratory of Fine Chemicals, Liaoning Key Laboratory for Catalytic Conversion of Carbon Resources, School of Chemical Engineering, Dalian University of Technology, Dalian 116024, P. R. China. E-mail: anhuilu@dlut.edu.cn;
Fax: +86-411-84986112; Tel: +86-411-84986112

† Electronic supplementary information (ESI) available. See DOI: <https://doi.org/10.1039/d2nj06030b>

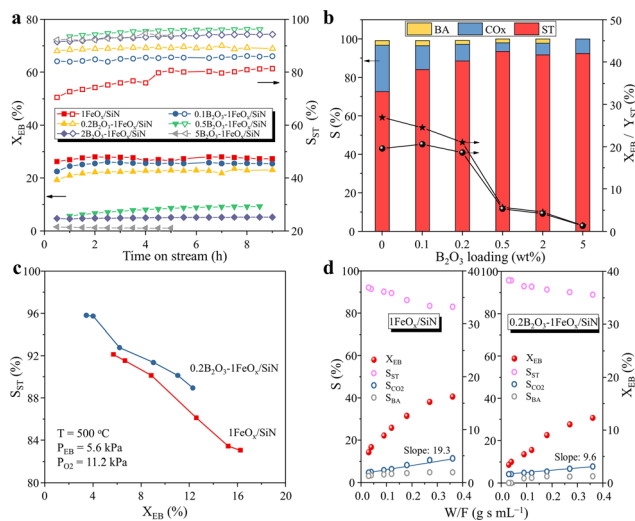


Fig. 1 The catalytic performance of $x\text{B}_2\text{O}_3\text{-1FeO}_x/\text{SiN}$ catalysts as a function of (a) time on stream and (b) B_2O_3 loading (data obtained at 1 h). Reaction conditions: $500\text{ }^\circ\text{C}$, $\text{EB} = 5.6\text{ kPa}$, $\text{O}_2/\text{EB} = 2$, N_2 as balance, $6000\text{ mL g}^{-1}\text{ h}^{-1}$. (c) Selectivity to styrene (S_{ST}) plotted as a function of ethylbenzene conversion (X_{EB}). (d) Effect of contact time on the catalytic behaviours in the ODH of EB. Reaction conditions: $500\text{ }^\circ\text{C}$, $\text{EB} = 5.6\text{ kPa}$, $\text{O}_2/\text{EB} = 2$, N_2 as balance, $9000\text{--}300\,000\text{ mL g}^{-1}\text{ h}^{-1}$.

to 5 wt% significantly influenced the catalytic performance, showing monotonically decreasing catalytic behaviour in terms of the conversion of ethylbenzene but increasing the selectivity of styrene. Among these catalysts, the $0.1\text{B}_2\text{O}_3\text{-1FeO}_x/\text{SiN}$ sample demonstrated a higher styrene yield, and the highest yield was found to be 20.6% and the selectivity of styrene was increased from 72 to 84%. As the loading of B_2O_3 increased to 0.5 wt% or 5 wt%, the conversion dramatically decreased to 5% or even to 1.5% (Fig. 1b), suggesting a prominent decrease in the number of active sites, probably due to the coverage of FeO_x species by excess B_2O_3 or the change of FeO_x species in physicochemical properties by modifying B_2O_3 . It is reported that B_2O_3 is not active in the oxidative dehydrogenation of ethylbenzene.⁸ These results indicated that a reasonable amount of B_2O_3 modification ($\sim 0.1\text{ wt\%}$) in $1\text{FeO}_x/\text{SiN}$ could improve the selectivity and yield of styrene, but excess B_2O_3 modification would lead to a decrease in ethylbenzene conversion and styrene yield.

To clarify that the increase in styrene selectivity with B_2O_3 modification was not affected by the conversion, the conversion-selectivity profile was tested. First, the absence of mass and heat transfer limitations was confirmed by the Weisz-Prater criterion (C_{WVP}) and Mears' criterion (C_{M}) (see ESI† for detailed calculation). As present in Fig. 1c, at the same conversion, the $0.2\text{B}_2\text{O}_3\text{-1FeO}_x/\text{SiN}$ was found to be more selective towards styrene than the $1\text{FeO}_x/\text{SiN}$ sample. As shown in Fig. 1d, the effect of the contact time (W/F) on the conversion of ethylbenzene to various products was further investigated. Over the $1\text{FeO}_x/\text{SiN}$ catalyst, the selectivity to styrene increased significantly to 93% and that to CO_x decreased to 5% as the contact time approached zero, suggesting that both styrene and

CO_x were the primary product. In contrast, over the $0.2\text{B}_2\text{O}_3\text{-1FeO}_x/\text{SiN}$ catalyst, the styrene selectivity increased to $\sim 98\%$ and the CO_x selectivity decreased to $\sim 2\%$ as the contact time decreased to zero. Thus, both styrene and CO_x were the major primary products. These results indicated the existence of direct oxidation of ethylbenzene to CO_x over both the $1\text{FeO}_x/\text{SiN}$ and $0.2\text{B}_2\text{O}_3\text{-1FeO}_x/\text{SiN}$ catalysts. The higher ultimate styrene selectivity ($\sim 98\% > 93\%$) observed over the $0.2\text{B}_2\text{O}_3\text{-1FeO}_x/\text{SiN}$ catalyst suggested that the overoxidation channels of direct oxidation of ethylbenzene to CO_x and the oxidation of styrene to CO_x were suppressed by the B_2O_3 modification. In addition, the slope between CO_x selectivity and contact time over the $0.2\text{B}_2\text{O}_3\text{-1FeO}_x/\text{SiN}$ was 9.6, much lower than that of $1\text{FeO}_x/\text{SiN}$ (19.3), which also reflected that the overoxidation reactions were suppressed over $0.2\text{B}_2\text{O}_3\text{-1FeO}_x/\text{SiN}$, leading to higher selectivity of styrene.

The XRD patterns of the $1\text{FeO}_x/\text{SiN}$ and $x\text{B}_2\text{O}_3\text{-1FeO}_x/\text{SiN}$ catalysts are shown in Fig. 2a. It can be seen that the $1\text{FeO}_x/\text{SiN}$ and $x\text{B}_2\text{O}_3\text{-1FeO}_x/\text{SiN}$ catalysts possessed a similar crystalline phase as that of the SiN support, probably due to the particle size of iron oxide being too small ($< 5\text{ nm}$) to be detected by XRD. Except in the $5\text{B}_2\text{O}_3\text{-1FeO}_x/\text{SiN}$ sample, no peaks of the crystalline B_2O_3 phase were observed in these modified samples, most probably due to the homogeneous dispersion of B_2O_3 . As shown in Fig. 2b, the dispersion of iron oxide (FeO_x) species was further studied by the UV-vis DRS technique (Fig. S1, ESI†). For clarity, the spectrum of the SiN support was subtracted from the UV-vis DRS spectra of the catalysts. The $1\text{FeO}_x/\text{SiN}$ and $x\text{B}_2\text{O}_3\text{-1FeO}_x/\text{SiN}$ could be attributed to the

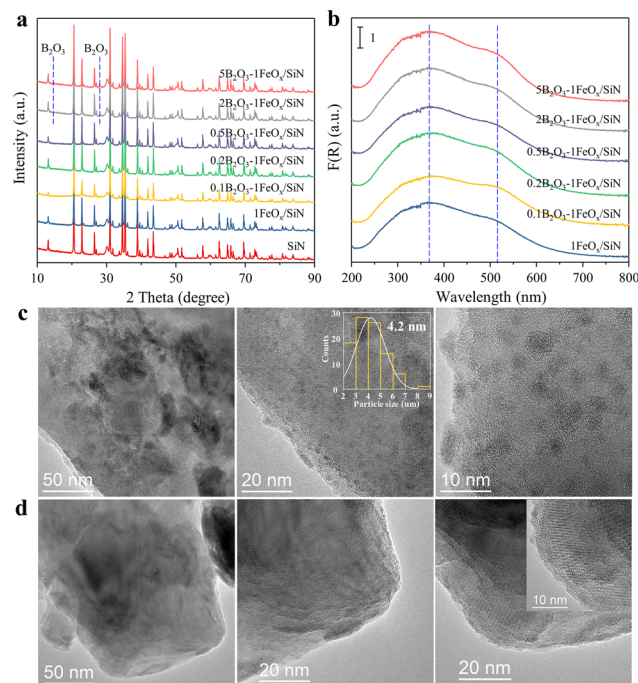


Fig. 2 (a) XRD patterns and (b) UV-vis DRS spectra for SiN and $x\text{B}_2\text{O}_3\text{-1FeO}_x/\text{SiN}$ samples. The spectrum of the SiN support was subtracted from the UV-vis DRS spectra of the catalysts. TEM images of the $1\text{FeO}_x/\text{SiN}$ (c) and $0.2\text{B}_2\text{O}_3\text{-1FeO}_x/\text{SiN}$ (d) samples.

ligand (O^{2-}) to metal (Fe^{3+}) charge-transfer (LMCT) transition for oligomeric FeO_x clusters.²⁰ The broad bands centered at 510 nm could be assigned to the crystalline Fe_2O_3 particles.²¹ TEM was further used to determine the distribution of FeO_x species from the micrology. As shown in Fig. 2c and Fig. S2 (ESI[†]), apparent FeO_x nanoparticles with a mean particle size of 4.2 nm were observed in the boron-free $1FeO_x/SiN$ sample. In contrast, a clear surface without nanoparticles was observed in the $0.2B_2O_3-1FeO_x/SiN$ sample (Fig. 2d and Fig. S3, ESI[†]). This phenomenon is also observed in other B_2O_3 -modified metal oxide catalysts, such as $B_2O_3-Co_3O_4/Al_2O_3$,¹³ B_2O_3-CuO/SiO_2 ,²² and $B_2O_3-CuZrO_2$.²³ More advanced characterization techniques, such as spherical aberration-corrected scanning transmission microscopy and EXAFS, will be helpful to understand the specific forms of ferrite species. Currently, the results of TEM indicate that the introduction of boron oxide could promote the dispersion of FeO_x species on the SiN support.

To investigate the interaction between FeO_x particles and the SiN support, H_2 -TPR experiments were performed and the corresponding results are shown in Fig. 3a. Three peaks located at 400, 470, and 640 °C were observed in the boron-free $1FeO_x/SiN$ sample, implying that the active component Fe_2O_3 underwent a stepwise reduction, which could be assigned to the reduction of Fe_2O_3 to Fe_3O_4 , Fe_3O_4 to FeO , and FeO to Fe ,²⁴ respectively. The reduction peak of the $x B_2O_3-1FeO_x/SiN$ with boric oxide modification shifted to higher temperatures with the increase in the boron loading, probably due to the chemical interaction between the iron oxide and the boric oxide becoming stronger. When the amount of boric oxide increased, gaining electrons during hydrogen reduction became harder for the iron oxide species because the electron affinity of boric oxide was higher than that of the SiN support.²⁵ The peak also tended to be widened with increasing boric oxide content, and one symmetric reduction peak at 645 °C was observed in the $5B_2O_3-1FeO_x/SiN$ sample. It is reported that smaller particles interacting strongly with the support were more difficult to be reduced,²⁴ indicating that the introduction of boron oxide could promote the dispersion of FeO_x species, consistent with the observation of TEM. The amounts of H_2 -uptake increased with the addition of B_2O_3 . However, a substantial drop in H_2 -uptake was found with increasing boron loading to 2 or 5 wt%, indicating that the excess B_2O_3 loading possibly covered the surface of FeO_x species and made it inaccessible to reacting hydrogen.²⁶

The dissociative adsorption of methanol is an effective method to determine the number of surface active sites on one-component metal oxide catalysts.²⁷ Here, the methanol oxidation product, formaldehyde (HCHO), is used to reflect the redox sites on these supported FeO_x catalysts.²⁷ As shown in Fig. 3b, two HCHO ($m/z = 30$) formation peaks at 107 and 258 °C were observed in the $1FeO_x/SiN$. With the modification of 5 wt% B_2O_3 , the HCHO formation temperatures increased to 167 and 419 °C. The much higher temperatures of HCHO formation in the $5B_2O_3-1FeO_x/SiN$ than that of the boron-free $1FeO_x/SiN$ sample suggested that boron modification would lower the redox reactivity of FeO_x species. The controllable oxygen

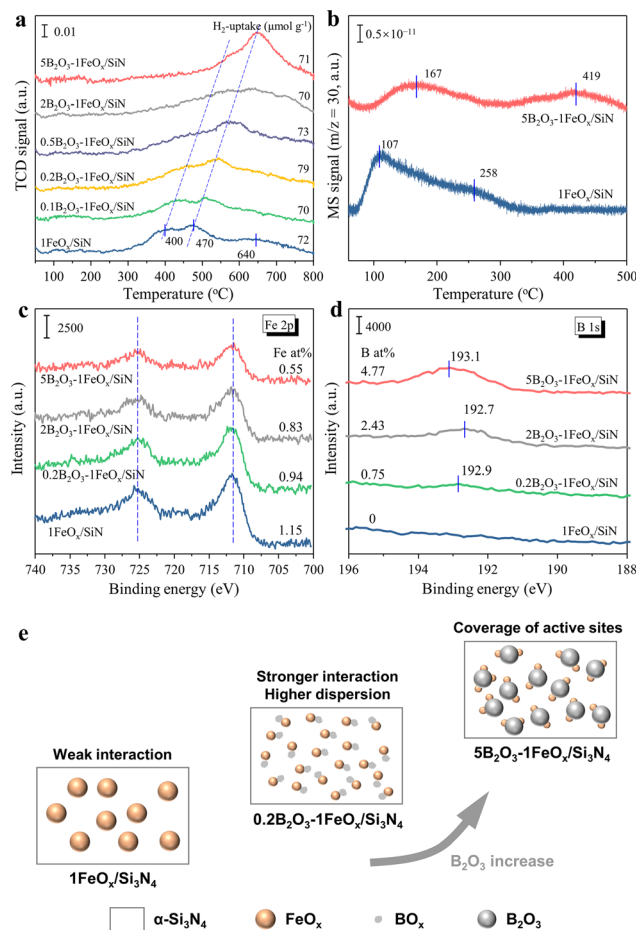


Fig. 3 (a) H_2 -TPR profiles for the $x B_2O_3-1FeO_x/SiN$ samples; (b) CH_3OH -TPD profiles of $1FeO_x/SiN$ and $5B_2O_3-1FeO_x/SiN$ samples. XPS spectra for $x B_2O_3-1FeO_x/SiN$ samples: (c) Fe 2p; (d) B 1s. (e) Schematic model of the FeO_x species on the SiN support with the increase of boron oxide.

reactivity of the FeO_x species showed a higher styrene selectivity in the oxidative dehydrogenation of ethylbenzene, consistent with the observation in our previous report.⁸

XPS was used to determine the surface composition and chemical state of calcined catalysts, as shown in Fig. 3c, d and Fig. S4 (ESI[†]). The Fe $2p_{3/2}$ and Fe $2p_{1/2}$ peaks (Fig. 3c) located at binding energies of 711.6 and 725.6 eV strongly suggested that the valence state of iron species was at the +3 after calcination. In Fig. 3d, the B 1s peak located at 192.7 to 193.1 eV was attributed to B^{3+} . A small shift of B 1s binding energy along with the same change in O 1s was observed (Fig. 3d and Fig. S4d, ESI[†]). Thus, we speculate this small shift was mainly caused by the difference of C 1s (surface carbon from contamination) over different catalysts. The increased peak intensity of B 1s indicated that the surface amount of B_2O_3 increased. The peak intensity of Fe 2p decreased with the increase in boron loading, and the surface amount of Fe was decreased from 1.15 to 0.55 at% with the introduction of 5 wt% B_2O_3 . These results implied the existence of B_2O_3 coverage on the FeO_x species.

Based on our results and the literature,²⁸ a possible schematic model of the catalysts was proposed as presented in

Fig. 3e. Characterization results demonstrated that the FeO_x species were poorly dispersed on the surface of the SiN support with a mean particle size of 4.2 nm at the loading of 1 wt% (Fig. 2c) and showed the strong redox reactivity of FeO_x species due to the weak interaction between the FeO_x species and support (Fig. 3a and b). When a small amount of boron oxide (0.2 wt%) was introduced into the catalyst, the dispersion of FeO_x species was promoted (Fig. 2d), but the redox reactivity of FeO_x species became lower because of the stronger interaction between the FeO_x species and BO_x species (Fig. 3a and b), showing higher styrene selectivity. However, excess boric oxide (0.5 to 5 wt%) loading led to the coverage of the exposed and accessible FeO_x species (Fig. 3a–d), and adversely affected the catalytic activity (Fig. 1a and b).

Conclusions

In summary, a series of B₂O₃-modified FeO_x/Si₃N₄ catalysts were prepared to investigate the role of the B₂O₃ additive and correlate the structure–performance relationship in the oxidative dehydrogenation of ethylbenzene. Based on the study of kinetics, H₂-TPR, and CH₃OH-TPD, it was revealed that the addition of B₂O₃ could mitigate the oxygen reactivity of FeO_x via the stronger interaction between the FeO_x and the BO_x species, which suppressed the overoxidation of ethylbenzene and styrene to carbon oxides. Also, the introduction of boron oxide could promote the dispersion of FeO_x species on the Si₃N₄ support. A moderate amount of B₂O₃ modification (0.1 or 0.2 wt%) could improve the selectivity and yield of styrene. Whereas excess B₂O₃ additive (0.5 to 5 wt%) would lead to the coverage of active FeO_x species, resulting in a decrease in ethylbenzene conversion and styrene yield. This B₂O₃ modification strategy can also be expanded into other heterogeneous catalytic systems, such as the preparation of other highly dispersed catalysts and the regulation of the chemical state of the active phase, optimizing the catalytic performance.

Author contributions

Jian Sheng: investigation, formal analysis, writing – original draft. Wen-Cui Li: formal analysis, conceptualization, writing – review & editing. Bai-Chuan Zhou: investigation, formal analysis. Xin-Qian Gao: formal analysis. Bin Qiu: formal analysis. Wen-Duo Lu: formal analysis. Rui-Ping Zhang: investigation. An-Hui Lu: conceptualization, supervision, funding acquisition, writing – review & editing.

Conflicts of interest

There are no conflicts to declare.

Acknowledgements

This study was supported by the State Key Program of the National Natural Science Foundation of China (21733002), and

the National Key Research and Development Project (2018YFA0209404 and 2021YFA1500300).

Notes and references

- 1 F. Cavani and F. Trifirò, *Appl. Catal., A*, 1995, **133**, 219–239.
- 2 S. Jarczewski, M. Drozdek, P. Michorczyk, C. Cuadrado-Collados, J. Gandara-Loe, J. Silvestre-Albero, L. Lityńska-Dobrzyńska and P. Kuśtrowski, *Appl. Surf. Sci.*, 2020, **504**, 144336.
- 3 J. Sheng, B. Yan, B. He, W.-D. Lu, W.-C. Li and A.-H. Lu, *Catal. Sci. Technol.*, 2020, **10**, 1809–1815.
- 4 W. Liu, B. Chen, X. Duan, K.-H. Wu, W. Qi, X. Guo, B. Zhang and D. Su, *ACS Catal.*, 2017, **7**, 5820–5827.
- 5 H. Ba, J. Luo, Y. Liu, C. Duong-Viet, G. Tuci, G. Giambastiani, J.-M. Nhut, L. Nguyen-Dinh, O. Ersen, D. S. Su and C. Pham-Huu, *Appl. Catal., B*, 2017, **200**, 343–350.
- 6 F. M. Bautista, J. M. Campelo, D. Luna, J. M. Marinas, R. A. Quirós and A. A. Romero, *Appl. Catal., B*, 2007, **70**, 611–620.
- 7 K. N. Rao, B. M. Reddy, B. Abhishek, Y.-H. Seo, N. Jiang and S.-E. Park, *Appl. Catal., B*, 2009, **91**, 649–656.
- 8 J. Sheng, W.-C. Li, W.-D. Lu, B. Yan, B. Qiu, X.-Q. Gao, R.-P. Zhang, S.-Z. Zhou and A.-H. Lu, *Appl. Catal., B*, 2022, **305**, 121070.
- 9 J. Sheng, W.-C. Li, Y.-R. Wang, W.-D. Lu, B. Yan, B. Qiu, X.-Q. Gao, S.-Q. Cheng, L. He and A.-H. Lu, *J. Catal.*, 2021, **400**, 265–273.
- 10 S. Chen, L. Zeng, R. Mu, C. Xiong, Z. J. Zhao, C. Zhao, C. Pei, L. Peng, J. Luo, L. S. Fan and J. Gong, *J. Am. Chem. Soc.*, 2019, **141**, 18653–18657.
- 11 J. Xu, B. Xue, Y.-M. Liu, Y.-X. Li, Y. Cao and K.-N. Fan, *Appl. Catal., A*, 2011, **405**, 142–148.
- 12 C. A. Carrero, R. Schloegl, I. E. Wachs and R. Schomaecker, *ACS Catal.*, 2014, **4**, 3357–3380.
- 13 M. Stranick, M. Houalla and D. Hercules, *J. Catal.*, 1987, **104**, 396–412.
- 14 J. Zheng, Z. Xia, J. Li, W. Lai, X. Yi, B. Chen, W. Fang and H. Wan, *Catal. Commun.*, 2012, **21**, 18–21.
- 15 J. Xu, L. Chen, K. Tan, A. Borgna and M. Saeys, *J. Catal.*, 2009, **261**, 158–165.
- 16 A. Fouskas, M. Kollia, A. Kambolis, C. Papadopoulou and H. Matralis, *Appl. Catal., A*, 2014, **474**, 125–134.
- 17 L.-L. Guo, J. Yu, M. Shu, L. Shen and R. Si, *J. Catal.*, 2019, **380**, 352–365.
- 18 I. Kurzina, F. Cadetesantosaires, G. Bergeret and J. Bertolini, *Chem. Eng. J.*, 2005, **107**, 45–53.
- 19 F. J. Cadete Santos Aires and J. C. Bertolini, *Top. Catal.*, 2009, **52**, 1492–1505.
- 20 P. Chen, M. Jabłońska, P. Weide, T. Caumanns, T. Weirich, M. Muhler, R. Moos, R. Palkovits and U. Simon, *ACS Catal.*, 2016, **6**, 7696–7700.
- 21 J. García-Aguilar, I. Miguel-García, J. Juan-Juan, I. Such-Basáñez, E. San Fabián, D. Cazorla-Amorós and Á. Berenguer-Murcia, *J. Catal.*, 2016, **338**, 154–167.
- 22 D. Yang, R. Ye, L. Lin, R. Guo, P. Zhao, Y. Yin, W. Cheng, W. Yuan and Y. Yao, *Nanomaterials*, 2021, **11**, 3236.

- 23 X. Zhang, Z. Duan, Y. Wu, T. Qiu and X. Shi, *Chem. Eng. Sci.*, 2021, **246**, 116897.
- 24 J. Wu, L. Wang, X. Yang, B. Lv and J. Chen, *Ind. Eng. Chem. Res.*, 2018, **57**, 2805–2810.
- 25 Z. He, H. Lin, P. He and Y. Yuan, *J. Catal.*, 2011, **277**, 54–63.
- 26 S. Singh, T. D. Nguyen, T. J. Siang, P. T. T. Phuong, N. H. Huy Phuc, Q. D. Truong, S. S. Lam and D.-V. N. Vo, *J. Energy Inst.*, 2020, **93**, 31–42.
- 27 M. Badlani and I. E. Wachs, *Catal. Lett.*, 2001, **75**, 137–149.
- 28 S. Zhao, H. Yue, Y. Zhao, B. Wang, Y. Geng, J. Lv, S. Wang, J. Gong and X. Ma, *J. Catal.*, 2013, **297**, 142–150.